

ENGINEERED FIBERS AND FABRICS

Original article

Effects of elasticity distribution on pressure and breast displacement for sports bras based on numerical simulation

Journal of Engineered Fibers and Fabrics Volume 20: 1–16 © The Author(s) 2025 DOI: 10.1177/15589250251352043 journals.sagepub.com/home/jef



Xiaofang Liu¹, Yue Sun², Xiaofen Ji^{3,4}, Kit-lun Yick⁵ and Liling Cai²

Abstract

Sports bras knitted with high-Young's modulus materials are effective in reducing the range of breast movement (ROM), but also increase the contact pressure to the body, leading to discomfort or even body injury. Elasticity distribution was found to be a factor influencing both pressure and ROM, however, the mechanism has yet to be studied, limiting its application in the sports bra industry. This study aimed to investigate the quantitative relationships between Young's modulus of different parts (C, S, S, B, U) and the performance metrics of sports bras in pressure and ROM for the optimization of both performance. A finite element (FE) model was developed to simulate the dynamic peak pressure at four test points and ROM for sports bras with different elasticity distributions during exercise. Based on which, a regression model was formed and the sensitivity factors (\$\phi\$) were ranked through 25 full factorial analysis. The results revealed that the influence of Young's modulus of each part varied with the pressure test points and the directions of ROM. Notably, the effect on pressure varied based on the placement of the test point relative to the part of sports bra. P₁, P₂, and P₄ were greatly influenced by Young's modulus of the part covering the test point and the parts nearby, whereas P_3 was mainly influenced by U. The effect on ROM predominantly depended on S_p C, and U rather than S_b and B. Therefore, the elasticity distribution design with relatively low S_b and B, relatively high S_f and U, and appropriate C was recommended to optimize both performances. These findings provide novel information for optimizing pressure comfort and breast support performance of sports bras, which is hoped to sever as a valuable reference for sports bra industry.

Keywords

elasticity distribution, pressure comfort, breast displacement, finite element method, sports bra

Date received: 21 October 2024; accepted: 7 June 2025

Hong Kong, China

Corresponding author:

Xiaofen Ji, College of Textile Science and Engineering (International Institute of Silk), Zhejiang Sci-Tech University, No. 928 2nd Street, Hangzhou, Zhejiang Province 310018, China.

Email: xiaofenji@zstu.edu.cn

 $^{^{\}rm I}$ College of Art, Jinling Institute of Technology, Nanjing, Jiangsu Province, China

²School of Fashion Design and Engineering, Zhejiang Sci-Tech University, Hangzhou, Zhejiang Province, China

³College of Textile Science and Engineering (International Institute of Silk), Zhejiang Sci-Tech University, Hangzhou, Zhejiang Province, China ⁴China National Silk Museum, Hangzhou, Zhejiang Province, China ⁵School of Fashion & Textiles, The Hong Kong Polytechnic University,

Introduction

Due to the limited anatomical support, women's breasts move relative to the trunk during exercise, which may result in exercise-related breast pain, the risk of breast sag and bad sports performance.²⁻⁴ Sports bra was reported to be effective in reducing breast movement, 5-9 therefore, researchers suggested women to wear sports bras during exercise to reduce breast movement. 1,2,5-9 Nevertheless, they also exert pressure on the human body due to the fabric tensile behavior of the sports bras, which may lead to discomfort, serious skin traces, or even heart, lung, and bowel function injury for the wearers. 5,6,10,11 Moreover, sports bras which were effective in reducing breast displacement often showed lower subjective pressure comfort, 7,12 or higher objective pressure. 8,13 As a result, pressure comfort and breast support performance emerge as two significant concerns for exercising women.

Literatures on sports bras revealed that both pressure and breast displacement were affected by the design features of sports bras, such as fabric, style, size, structure, and so on. 5,8,9,14-21 Among them, Young's modulus (*E*), which is used to measure fabric deformation under external force (calculated as tensile stress divided by tensile strain), 9 was recognized as a critical determinant. 5,8,9,14,16-18 However, in the studies concentrated on the effects of Young's modulus, 5,8,9,14,16-18 researchers 5,8,16,17 either focused on the effects of Young's modulus on pressure, or investigated the effects on ROM, 9,14,18 few addressed the effects both on pressure comfort and ROM.

Elasticity distribution, that is, applying fabrics with different Young's modulus in different areas, ¹⁹ was often used to improve pressure comfort and other performance of the garments. For example, it was found that compression shaping pants knitted with different structures and thickness in different area performed graduated pressure and promoted blood microcirculation of lower limbs. ²⁰ Knitwear by careful control of elasticity distribution was effective in reducing uncomfortable pressure and unwanted

sliding caused by body motion. ¹⁹ Recently, researchers found bra with high Young's modulus in the side area of the under-band was ideal both in pressure comfort and breast support performance. ²¹ It implied that appropriate elasticity distribution was effective in both pressure and breast support. However, since the study only examined four elasticity distribution cases in the under-band, the effects of elasticity distribution of the whole sports bra have not been investigated, that is, the effects of Young's modulus of other parts (such as strap, cup, and back panel) and their interactions on the pressure of other body parts and breast displacement have not been revealed, limiting its application in the optimization of the pressure comfort and breast support performance of sports bras.

The quantitative relationships between Young's modulus of each part and the performance metrics of pressure and the range of breast movement (ROM), which is used to evaluate breast movement and calculated by subtracting the trough position value from the consecutive peak position value of breast test point), 14,22,23 forms the basis for optimizing both performance. Consequently, this study aimed to investigate the relationships between young's modulus of different parts of sports bras (front strap, back strap, cup, back panel and under-band, as shown in Figure 1) and the performance metrics of pressure and ROM. Given that traditional experimental methods are often time-consuming, labor-intensive, and susceptible to random factors, a finite element model was developed to simulate the pressure and ROM of women wearing sports bras with different elasticity distribution during exercise, based on which, regression model were formed through 25 full factorial analysis, and the influence of elasticity distribution on pressure of four test points and ROM was discussed.

Finite element method (FEM), that is, a numerical approach to solve practical problems by conducting simulations, ²⁴ is widely applied to establish dynamic models of human body and garments, to evaluate the contact pressure, the deformation and the displacement of body parts, and the heat transaction beneath the garments, demonstrating

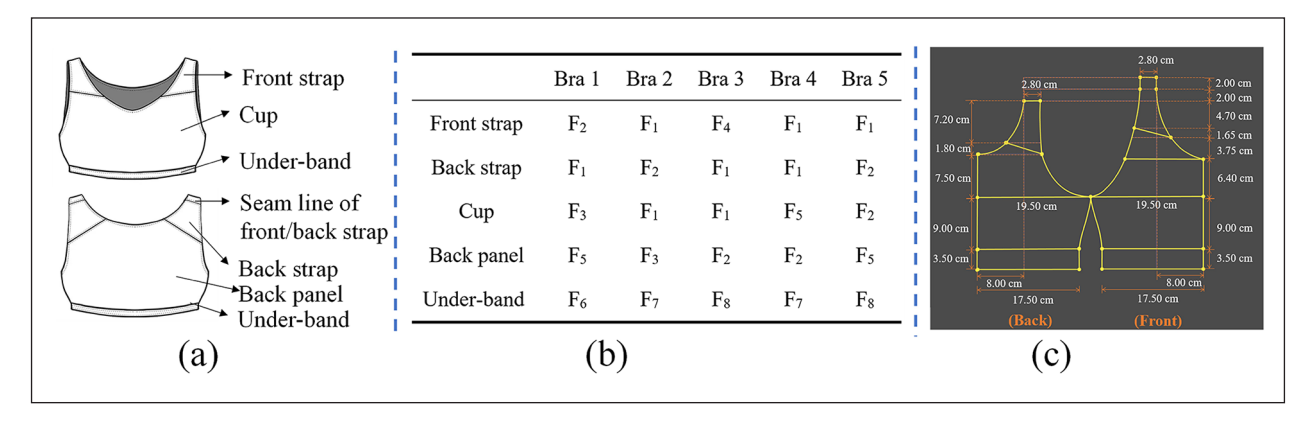


Figure 1. Experimental samples: (a) elasticity distribution illustration, (b) fabrics used for samples, and (c) dimensional specifics.

considerable robustness in previous researches.^{24–29} For example, Sun et al.²⁵ proposed an Optimization method for the determination of Mooney-Rivlin material coefficients of the human breasts by applying static and dynamic FE models. Zhang et al.²⁴ developed a novel method to simulate the interaction of the bra strap and the movement of upper body, provided effective design modifications for today's everchanging lingerie market. Chen et al.²⁶ established a novel nonlinear multi-component dynamic finite element method to explore the biomechanical behavior and the stiffness impact of the breast internal components during running.

We hoped the results of this paper would provide novel information in the optimization of the pressure comfort and breast support performance for researchers in sports bras, benefiting the sports bras industries and exercising women.

Methodology

A dynamic bra-body contact FE model was built in this part, based on which, a factorial analysis method was proposed, and the process in this section includes following steps:

- (1) Experiment: physical property testing, pressure testing and motion capturing experiment for constructing and validating the FE model;
- (2) FE model construction: geometric model established by using three-dimensional scanning and reverse engineering, and contact model constructed based on the results of the experiments;
- (3) 2⁵ full factorial experiment design: full factorial analysis method designed based on the FE model.

Experiment

Participant. Elder Women with more ptotic breasts and whose skin overlying the breasts and Cooper's ligament becomes less elastic, needs more breast support provided externally by sports bras to compensate for their reduced anatomical support during exercise. 30 Therefore, following institutional ethical approval, a 63-yearold Chinese healthy female subject (height: 159.75 cm, weight: 62.39 kg, bust girth: 97.21 cm, under-bust girth: 84.62 cm, bra size: 85B) was recruited as participant, whose anthropometric measurements fell within the average range of Chinese elder women observed in a survey of 115 Chinese elder women.³¹ The participant had gone through pregnancy, breast feeding, menopause, experienced no surgical procedures to the breasts, and undertook ≥30 min of exercise more than four times a week.

Experiment samples. Five compression sports bras with different elasticity distribution were used as experiment

samples, for their wide straps, sufficient vertical cup length, increased gore height, and underarm height were proved to be effective in well-fitting for elder women.³² The sports bras consisted of five parts, namely front strap, back strap, cup, back panel, and under-band. As the top point of shoulder (one of the pressure test points in this study, as shown in Figure 2) might slip between the front strap and back strap during exercise, the front strap was extended 2 cm backwards to make sure that the top point of shoulder was always covered by the front strap. The only differences among these five sports bras were the elasticity distribution, other than these differences, the style, structure, size, and production methods were kept same. The circumference of under-band and that around the bust were set as 70 and 78 cm respectively, and the vertical height of the sports bra was set as 31 cm, according to previous researches and the sports bra market. 18,32 The dimensions of other parts were specified in Figure 1, the pattern was created in Style 3D Studio (Linctex, China), and the sewing process was carried out using an interlock machine (Solay, China).

Eight widely-used elastic fabrics were applied for the elasticity distribution of the samples, of which F_6 , F_7 , and F_8 were ribbed fabrics, used in the under-band, and the others (F_1-F_5) were used in the other parts of the samples (Figure 1).

Material test. Young's modulus of eight fabrics were tested with Instron 3365 (Instron, USA), based on FZ/T 70006-2004. As the under-band of the samples were double layers, the ribbed fabrics (F_6-F_8) were folded and sewn into double-layer strips for tensile testing to simulate the real wearing conditions of the under-bands. A high-definition camera (SONY, Japan) and Adobe Illustrator (Adobe, USA) was used to record and measure the length and width of the fabric samples during the stretching process for the calculation of Poisson's ratio (p). The density test was carried out with an electronic balance (XingYun, China), and the thickness was tested with a fabric thickness tester (YG, China). The physical properties of the fabrics (F_1-F_8) were summarized in Table 1.

Pressure test. Four points were chosen as the pressure test points, that is, the top point of shoulder (P_1) , the midpoint of the top area of scapular (P_2) , intersection point of underband and side seam (P_3) , the midpoint between lateral breast root and the bottom of the breast (P_4) , as shown in Figure 2. P_1 and P_2 were always reported for the pressure discomfort, 20,33,34 while P_3 and P_4 were selected based on the bending shape in the top area of scapula resulted from kyphosis, and the sagging and lower-lateral extending breasts of the elder women. 35

The dynamic peak pressure were tested with a pressure testing system (MFF, China), with the pressure sensors (FlexiForce, USA) attached to four points (Figure 2). Due

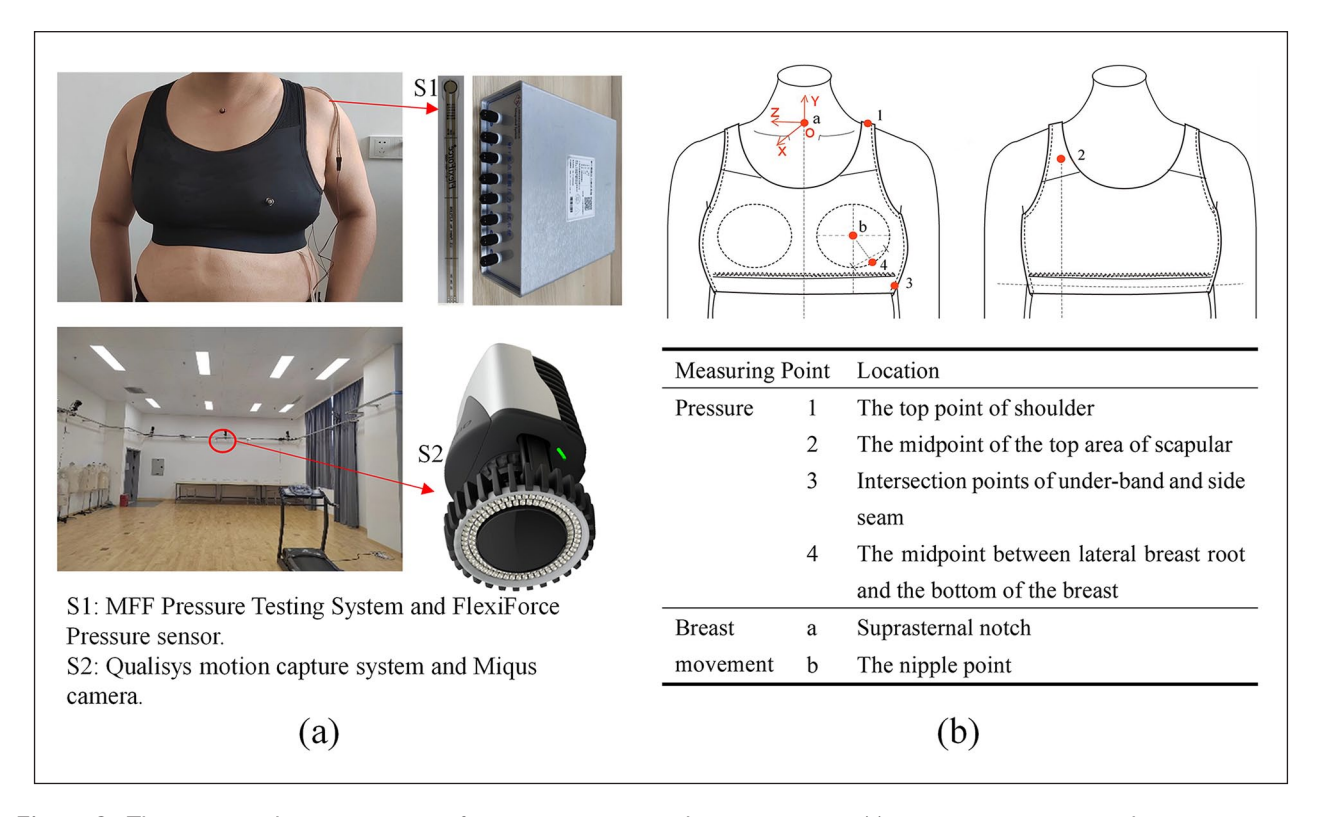


Figure 2. The system and measuring points for pressure testing and motion capture: (a) pressure test system and motion capture system and (b) pressure and ROM test points.

Table 1. Physical property summary of the fabrics for five sports bras.

Fabric	Fabric content	Density (g/m²)	Thickness (mm)	E (MPa)	Þ
F,	53.1% polyester, 33.5% polyamide, 13.4% spandex	230.9	0.804	1.6761	0.22
F ₂	88.2% polyester, 12.8% spandex	310.2	0.831	2.5132	0.17
F ₃	69.1% polyester, 21.9% polyamide, 9.0% spandex	220.2	0.783	1.3429	0.25
F ₄	89.3% polyester, 10.7% spandex	305.6	0.822	3.1025	0.08
F ₅	82.2% polyester, 17.8% spandex	251.5	0.811	0.6328	0.29
F ₆	69.1% polyester, 21.9% polyamide, 9.0% spandex	559.9	1.618	2.5573	0.07
F ₇	52.8% polyester, 33.6% polyamide, 13.6% spandex	495.4	1.588	1.3431	0.09
F ₈	64.6% polyester, 23.8% cotton, 8.7% spandex	547.5	1.565	2.1223	0.08

The results of F_6 – F_8 were obtained from the tests in which fabrics were folded into double-layer to simulate the real wearing conditions of the under-bands.

to the decline of exercise capabilities, high-intensive activities, such as running, is not suitable for elderly women as daily exercise. Instead, Square Dance is a highly recommended and widely popular exercise among elderly women in China.³⁶ As a result, a typical motion of square dance, that is, forwards-backwards stepping (Figure 3), was chosen as the experimental action. As the deformation of the breasts caused by arm movements might affect the experiment results, the subjects were required to put their hands on their waist. A 30-cycles duration at a frequency of 23 cycles/minute (the pace was controlled by a dancing music) was chosen for the experiment, and the middle

consecutive 10 gait cycles (the 11th–20th) were chosen for analysis. Each sample was tested five times, and the mean dynamic peak pressure was taken as the average of the peak pressure in total 50 gait cycles (10 gait cycles multiplied by five times).

Motion capture. The motion capture experiment was carried out simultaneously with the pressure test, and the motion of the breast when wearing five sports bras in ground coordinate system (GCS) was captured by the motion capture system (Qualisys, Sweden). According to biomechanical researches, breasts will move in three

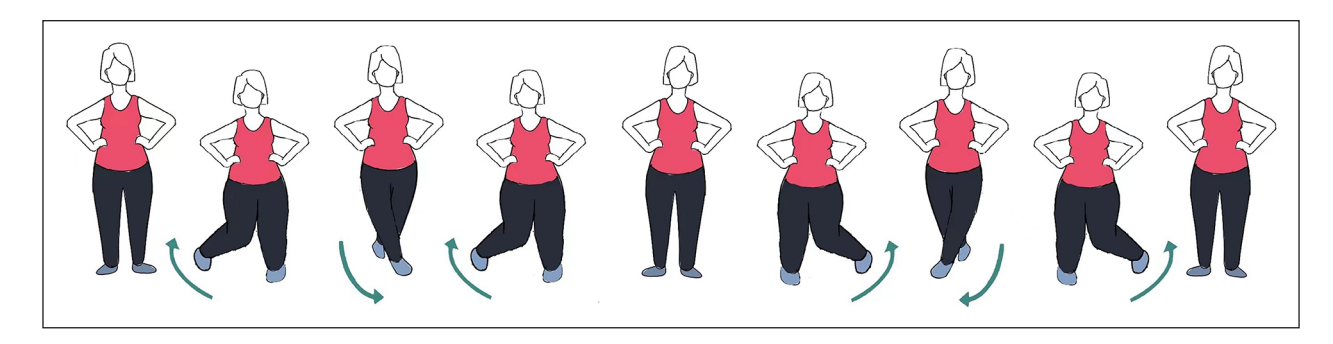


Figure 3. The illustration of the experimental motion: forwards-backwards stepping.

directions relative to the trunk during exercise.¹ As the trunk also moves during exercise, it is necessary to construct a trunk local coordinate system (LCS) to convert the displacement data of breast in GCS to the data in LCS.

During forwards-backwards stepping, as the torso mainly moves in anterior-posterior and vertical direction with little rotation, LCS based on the reference point of suprasternal notch which was proved to be of high accuracy in exercises where trunk predominantly translated with little rotation (such as running and jumping)^{8,13,15,28,37} was established (*x*: anterior-posterior, *y*: vertical, *z*: medial-lateral, the origin of the LCS: suprasternal notch), as shown in Figure 2. The nipple which was recommended as a representative measuring point of breast was chosen for the breast movement testing.^{8,13–15,21} The relative breast displacement (in LCS) was calculated by subtracting the displacement data of the suprasternal notch from that of the nipple.¹⁵

Two retro-reflective markers were attached to these two points, that is, the suprasternal notch (as the reference point) and the nipple (as the breast movement measuring point). Similarly, the middle consecutive 10 gait cycles (the 11th–20th) were chosen for analysis. And the mean ROM after wearing each sports bra was taken as the average of the ROM in 50 gait cycles (10 gait cycles multiplied by five times).

FE model construction

Geometric model. A Non-contact three-dimensional human scanner ((TC),² USA) was used for the image of the participant, and the reverse engineering software, that is, Geomagic Wrap and Geomagic Design X (3D Systems, USA), were applied for constructing the geometric model of the trunk. For the simulating efficiency of the FE model, the trunk (consisted of several parts, such as skin, muscles, adipose tissue, vessel, bones, lungs, and heart) was simplified to three main parts: the torso, the soft tissue, and the breasts. The thickness of the soft tissue was set as 2.30 cm, according to the average thickness of soft tissue in the front part of the trunk (Figure 4). The geometric model of the body was meshed with four-node tetrahedral elements, as its quadratic displacement behavior is quite suitable for

the modeling of the irregular shape deformation often found on the female breast.³⁹ The geometric model of the sports bra was extracted from the model of the body, and divided into five parts (front strap, back strap, cup, back panel, and under-band). Finally, 6 mm tetrahedral elements were applied for the meshing, based on the accuracy and efficiency of calculation time.

Material properties. A Mooney-Rivlin material model with five coefficients (C₁₀, C₀₁, C₁₁, C₀₂, and C₂₀), which has been proven to be effective in simulating large deformations and nonlinear mechanical behaviors of breasts⁴⁰ was applied to construct the breast model with a FE analysis software (MSC Marc, USA). The initial coefficients of the breasts (C_{10} =0.094 kPa, C_{01} =0.108 kPa, C_{11} =0.820 kPa, C_{02} =1.180 kPa, C_{20} =0.840 kPa)²⁸ were set and multiplied by a series of compensation factor $\alpha(0.875, 0.750, 0.625,$ 0.500, 0.375) to get different coefficients. The differences between ROM (without bras) in the experiment and that simulated by the FE model with different coefficients were compared and minimized based on root mean squared error (RMSE), which was calculated with formular (1).25,28,41 Finally, the coefficients : C_{10} =0.071 kPa, C_{01} =0.081 kPa, C_{11} =0.615 kPa, C_{02} =0.885 kPa, C_{20} =0.630 kPa (α =0.750) with the lowest RMSE in three directions (RMSE = 0.22, RMSE, = 0.32, RMSE, = 0.36) were selected for the model.

$$RMSE = \frac{1}{n} \sqrt{\sum_{i=1}^{n} \left(\frac{ROM_{exp,i} - ROM_{fem,i}}{ROM_{exp,i}} \right)^{2}} \times 100\%$$
 (1)

Where $ROM_{exp,i}$ is the range of breast movement tested in the experiment in three directions respectively, while $ROM_{fem,i}$ denotes the range of breast movement simulated by the FE model in the corresponding direction, and n refers to the number of sample data points.

For the damping ratio (ζ) of breasts, the method of a free vibration developed by Cai et al.⁴² was adopted and modified. The subject was asked to raise one of her breasts and hold it for 5 s. Then, removed her hand quickly to let the breast fall freely due to the breast mass and inertia. The damping ratio (ζ) was calculated as follows⁴²:

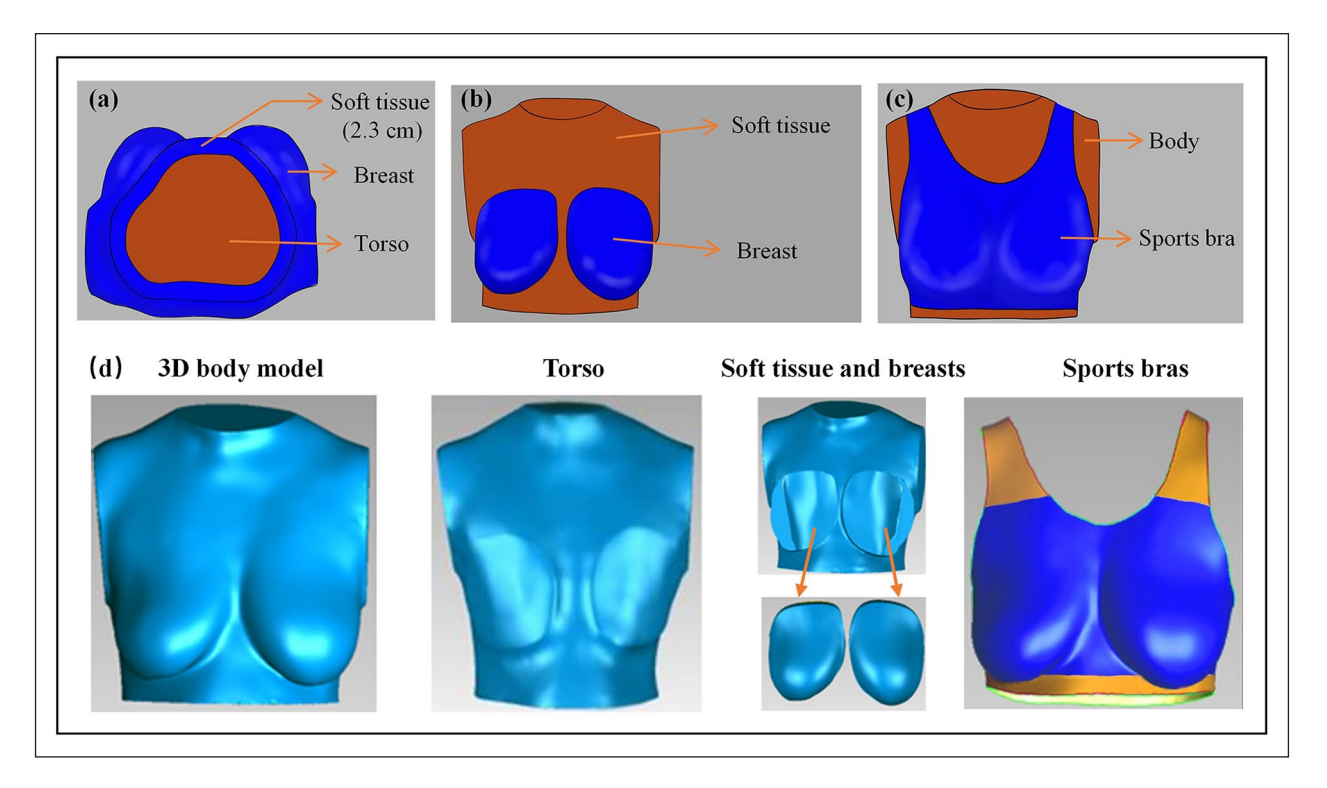


Figure 4. Geometric models for torso, soft tissue, breasts, and sports bra.

Table 2. Material parameters of the FE model of breast.

Coefficient of Mooney-Rivlin model (kPa)						
C ₁₀	C ₀₁	C _{II}	C ₁₁ C ₀₂ C ₂₀		Damping ratio ζ	ρ (kg/m ³)
0.071	0.081	0.615	0.885	0.630	0.268	950

Table 3. Material parameters of the FE models of soft tissue and torso.

Components	Parameters	Value
Soft tissue	C ₁₀ (kPa)	5
	C ₀₁ (kPa)	5
	ρ (kg/m ³)	1000
Torso	E (GPa)	9.8
	Poisson's ratio p	0.3
	ρ (kg/m³)	1800

$$\zeta = \frac{\delta}{\sqrt{(2\pi)^2 + (\delta)^2}} \tag{2}$$

$$\delta = \ln\left(\frac{y_n}{y_{n+1}}\right) \tag{3}$$

Where δ denotes the logarithmic decrement, y_n is the amplitude at the nth peak of the damped waveform. The density of breasts was set as $950 \, \mathrm{kg/m^3}$, according to the

average breast density of elder women,^{25–27} and the material properties of breast were summarized in Table 2.

A Mooney-Rivlin material model with two coefficients was selected to construct the soft tissue model,²⁵ while the mechanical behavior of the torso was regarded as isotropic, and the material properties were set according to previous researches,^{29,43} as shown in Table 3.

The FE model of sports bra fabric is assumed to be isotropic, and the Young's modulus (E), the Poisson's ratio (p), and the density (ρ) of every part were calculated from the data acquired by the experiment, as shown in Table 1. Interaction through contact was established for bra-body contact, whereas interaction through glue was established for torso-soft tissue contact and soft tissue-breast contact.

Loading and boundary conditions. As the geometric model of the body was initially based on the subject in a standing position with gravity, a force with the same magnitude as gravity yet in the opposite direction was added to the breast in order to construct a static equilibrium position of the breasts. Subsequently, the boundary conditions of thermal expansion, breast loading, and the torso movement were applied to the model according to the following steps:

(1) To simulate the fabric tension behavior of sports bra after wearing, a thermal expanding boundary condition was applied to simulate the actual contact condition between the sports bras and the human body. Firstly, the size of the original models of the body and bra were geometrically reduced in each direction (X, Y, and Z). Secondly, reduce the body model again, until a gap between the models of the body and the sports bra was noted (the volume of the body was noted as V_0). Thirdly, expanded the model of the body in three directions with a thermal expansion coefficient (formular (4)) until the size of the body model reached the original size before reducing. Finally, the model of the sports bra was expanded with the body to the actual size after wearing, and the contact stress generated due to the fabric elongation.

$$\alpha_V = \frac{1}{V_0} \frac{\Delta V}{\Delta T} \tag{4}$$

where α_v is the volumetric coefficient of the thermal expansion, ΔV is the variation in the model size of the body, V_0 denotes the volume of the body after the second reducing, and ΔT is the temperature variation.

- (2) Apply a downward gravity acceleration (-9800 mm/s²) to the nodes of the breast model for the simulation of the gravity.
- (3) Apply torso displacement acquired in the experiment onto the torso to simulated the body motion.

The research process of the FE model construction was shown in Figure 5.

2⁵ Full factorial experiment design

A two-level full factorial DOE was used to explore the influence of the elasticity distribution on the dynamic peak pressure of four test points and ROM, and the Young's modulus of five bra parts was inputted as the varying factors.

The Young's modulus of the fabrics used in the straps, cups, and back panels of sports bras usually varied from 0.20 to 3.10 MPa (average: 1.65 MPa), according to previous researches and the sports bra market. 8,24,41 As a result, the Young's modulus of F_1 (1.6167 MPa), which was closest to the average value of 1.65 MPa was set as the nominal value (denoted as 0), with 0.2761 MPa as low level (denoted as -1), and 3.0761 MPa as high level (denoted as +1). Similarly, The Young's modulus of ribbed fabrics used in the under-band of sports bras usually varied from 1.30 to 3.80 MPa (average: 2.55 MPa). 8,24,41 Consequently, 2.5573 MPa of F_6 was set as the nominal value (denoted as 0), with 1.3673 MPa as low level (denoted as -1), and

 $3.7473 \,\mathrm{MPa}$ as high level (denoted as +1), as shown in Table 4.

Results and discussion

The results of the FE model validation and 2^5 full factorial analysis were discussed in this section. The dynamic pressure at four test points and ROM obtained from the experiments were compared with that simulated by the FE model for validation. Subsequently, the validated model was employed to simulate of output responses in the 2^5 full factorial analysis. Based on which, the quantitative relationships between varying factors (Young's modulus of five parts and their interactions) and the output responses (dynamic pressure at four points and ROM) were elucidated through regression model, and the elasticity distribution for optimizing pressure comfort and breast support performance were discussed according to the ranking of normalized sensitive factor φ .

FE model validation

Pressure comparison. The dynamic peak pressure of four test points simulated by the FE model was compared to the experiment results, and RMSE of dynamic peak pressure (RMSE_p, formular (5)) was taken for validating the reliability of an FE model.^{25,28,41}

$$RMSE_{P} = \frac{1}{n} \sqrt{\sum_{i=1}^{n} \left(\frac{P_{exp,i} - P_{fem,i}}{P_{exp,i}} \right)^{2}} \times 100\%$$
 (5)

Where $P_{\exp,i}$ is the dynamic peak pressure in gait cycle "i" in the experiment, whereas $P_{fem,i}$ refers to the dynamic peak pressure in gait cycle "i" simulated by the FE model.

As shown in Table 5, RMSE of Points 1, 2, and 4 were low (0.334%–0.679%), while Point 3 exhibited a little higher RMSE than the other points (0.885%, 0.838%, 0.887%, 0.856%, 0.851% respectively for Bra 1–Bra 5). This might have been caused by the differences between the setting of single-layer for the under-band in the FE model and the actual double-layer in the experiment. Slippage between these two layers might have occurred during the experiment, which was not simulated in the FE model. Overall, RMSE of four points was all below 1%, which could be considered as receptive. ^{25,28,41}

Comparison of breast displacement. Figure 6 shows the experimental and simulated breast displacement in three directions in one typical gait cycle, when the subject wearing five sports bras. Generally, the breast displacement simulated by the FE model showed a similar trend to that obtained in the experiment, of which a regular periodic variation with four stages

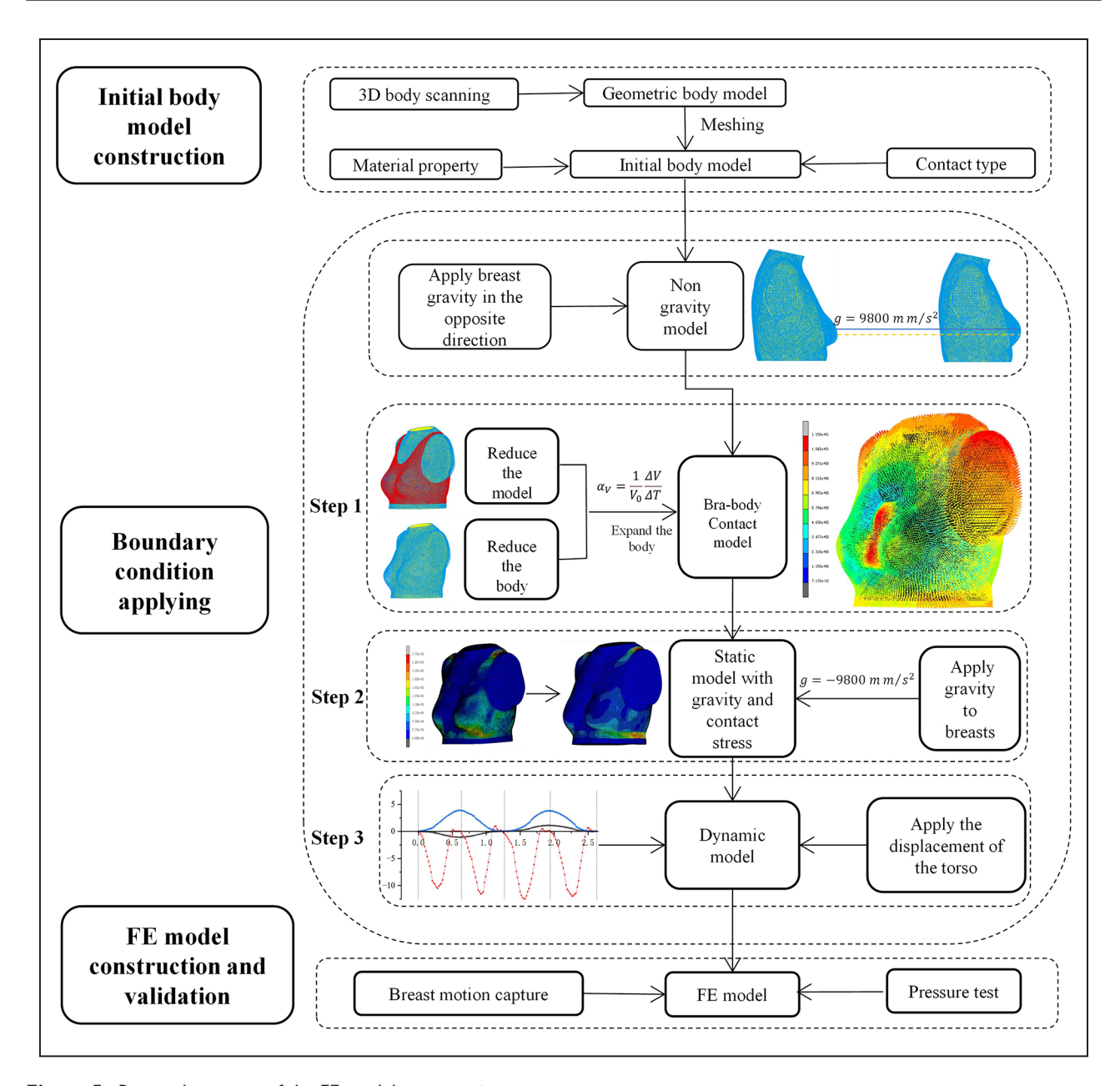


Figure 5. Research process of the FE model construction.

Table 4. 2⁵ Full factorial experiment design.

	Low level	Nominal value	High level
Factors	-1	0	1
C (MPa)	0.2761	1.6761	3.0761
S _f (MPa)	0.2761	1.6761	3.0761
S _b (MPa)	0.2761	1.6761	3.0761
B (MPa)	0.2761	1.6761	3.0761
U (MPa)	1.3673	2.5573	3.7473

C: Young's modulus of the cup; S_r : Young's modulus of the front strap; S_p : Young's modulus of the back strap; B: Young's modulus of the back panel; U: Young's modulus of the under-band.

in one gait cycle was observed. RMSE for Bra 4 (calculated by formular (1)) was 0.836%, 0.891%, 0.793% for *X*, *Y*, and *Z* directions respectively, a little higher than other bras (0.338%–0.608%). It might have been due to the differences in breast lifting position after wearing five sports bras. It was observed in the experiment that the nipple position after wearing Bra 4 was much lower than others, which might have been caused by the much lower Young's modulus of the cup fabric for Bra 4 (0.6328 MPa). Nevertheless, the nipple height in the FE model was the same based on the same geometric model, resulted in a higher RMSE for Bra 4. The results suggested full considerations of the differences between bras when constructing the FE geometric model in

Table 5.	Comparison of	the dynamic pea	k pressure at 1	four test points.

Samples	Dynamic peak pressure	Point I	Point 2	Point 3	Point 4
Bra I	P _{exp} (kPa)	3.30 ± 0.23	1.82 ± 0.13	2.71 ± 0.22	1.21 ± 0.09
	P _{fem} (kPa)	$\textbf{3.17} \pm \textbf{0.25}$	$\textbf{1.89} \pm \textbf{0.12}$	$\textbf{2.88} \pm \textbf{0.12}$	$\textbf{1.16} \pm \textbf{0.10}$
	RMSE (%)	0.557	0.542	0.885	0.581
Bra 2	P _{exp} (kPa)	$\pmb{2.97 \pm 0.21}$	$\textbf{2.23} \pm \textbf{0.18}$	$\textbf{2.02} \pm \textbf{0.15}$	$\textbf{1.27} \pm \textbf{0.08}$
	P _{fem} (kPa)	$\textbf{3.06} \pm \textbf{0.27}$	2.13 ± 0.19	1.90 ± 0.11	$\textbf{1.22} \pm \textbf{0.12}$
	RMSE (%)	0.421	0.632	0.838	0.551
Bra 3	P _{exp} (kPa)	3.77 ± 0.29	2.47 ± 0.13	2.86 ± 0.22	$\textbf{1.69} \pm \textbf{0.07}$
	P _{fem} (kPa)	3.66 ± 0.30	2.39 ± 0.16	2.68 ± 0.18	1.61 ± 0.09
	RMSE (%)	0.412	0.457	0.887	0.667
Bra 4	P _{exp} (kPa)	2.76 ± 0.18	2.08 ± 0.16	2.07 ± 0.15	$\textbf{1.04} \pm \textbf{0.09}$
	P _{fem} (kPa)	2.64 ± 0.22	2.16 ± 0.12	1.94 ± 0.14	0.99 ± 0.08
	RMSE (%)	0.580	0.570	0.856	0.679
Bra 5	P _{exp} (kPa)	$\textbf{3.38} \pm \textbf{0.23}$	2.11 ± 0.17	2.65 ± 0.21	$\textbf{1.37} \pm \textbf{0.07}$
	P _{fem} (kPa)	3.46 ± 0.28	2.04 ± 0.13	2.49 ± 0.13	$\textbf{1.42} \pm \textbf{0.09}$
	RMSE (%)	0.334	0.468	0.851	0.515

 P_{exp} : dynamic peak pressure obtained from the experiment; P_{fem} : dynamic peak pressure simulated by the FE model; RMSE: root mean squared error between P_{exp} and P_{fem} .

future studies. Moreover, RMSE for five sports bras was all within 1%, which indicated that the simulated results were acceptable. 25,28,41

Regression model of output response

As a 2⁵ full factorial experiment, 32 tests (with three center points) in the combinations of Young's modulus of five parts at two levels were conducted. The corresponding results (the dynamic peak pressure of four points and ROM in three directions) for each test were simulated by the validated FE model, and the design matrix of varying parameters and the output response for each test were shown in Table 6.

The factorial analysis was conducted in Minitab statistical software (Minitab, USA). As high-order terms were not illustrative and practical for sports bra manufacturers, only main effects and second-order interaction effects with significance were retained in the regression model. Equations following showed the quantified relationships between the dynamic peak pressure at four test points and Youngs' modulus of five parts and their interactions.

$$\begin{split} P_1 &= 0.577 + 0.350 \left\langle C \right\rangle + 0.502 \left\langle S_f \right\rangle + 0.145 \left\langle U \right\rangle \\ &+ 0.336 \left\langle S_b \right\rangle + 0.065 \left\langle B \right\rangle - 0.072 \left\langle CS_f \right\rangle \\ &+ 0.055 \left\langle S_f S_b \right\rangle \end{split} \tag{6}$$

$$P_2 = 0.360 + 0.054 \langle C \rangle + 0.129 \langle S_f \rangle + 0.063 \langle U \rangle$$

$$+0.447 \langle S_h \rangle + 0.213 \langle B \rangle + 0.027 \langle S_h B \rangle$$

$$(7)$$

$$P_3 = 0.450 + 0.056 \langle C \rangle + 0.055 \langle S_f \rangle + 0.828 \langle U \rangle$$

$$+0.038 \langle S_h \rangle + 0.086 \langle B \rangle$$
(8)

$$P_4 = 0.119 + 0.269 \langle C \rangle + 0.142 \langle S_f \rangle + 0.067 \langle U \rangle$$

+0.038\langle S_h \rangle + 0.120 \langle B \rangle + 0.036 \langle CB \rangle
$$(9)$$

And the numerical relationships between ROM in three directions and the varying factors were shown as follows.

$$ROM_{x} = 1.746 - 0.101 \langle C \rangle - 0.144 \langle S_{f} \rangle - 0.078 \langle U \rangle$$
$$-0.020 \langle S_{b} \rangle - 0.008 \langle B \rangle - 0.012 \langle CS_{f} \rangle$$
(10)

$$ROM_{y} = 5.505 - 0.343 \langle C \rangle - 0.598 \langle S_{f} \rangle$$

$$-0.449 \langle U \rangle - 0.128 \langle S_{b} \rangle - 0.070 \langle B \rangle$$
(11)

$$ROM_{z} = 2.284 - 0.215 \langle C \rangle - 0.176 \langle S_{f} \rangle$$
$$-0.121 \langle U \rangle - 0.023 \langle S_{b} \rangle - 0.038 \langle B \rangle$$
(12)

Where P_1-P_4 refers to the dynamic peak pressure of Point 1-Point 4, and ROM_x , ROM_y , and ROM_z denotes the breast displacement in direction X, Y, and Z. C, S_p , U, S_b , B refers to Young's modulus of cup, front strap, under-band, back strap, and back panel respectively, while CS_p , S_fS_b , were the interactions of two corresponding factors.

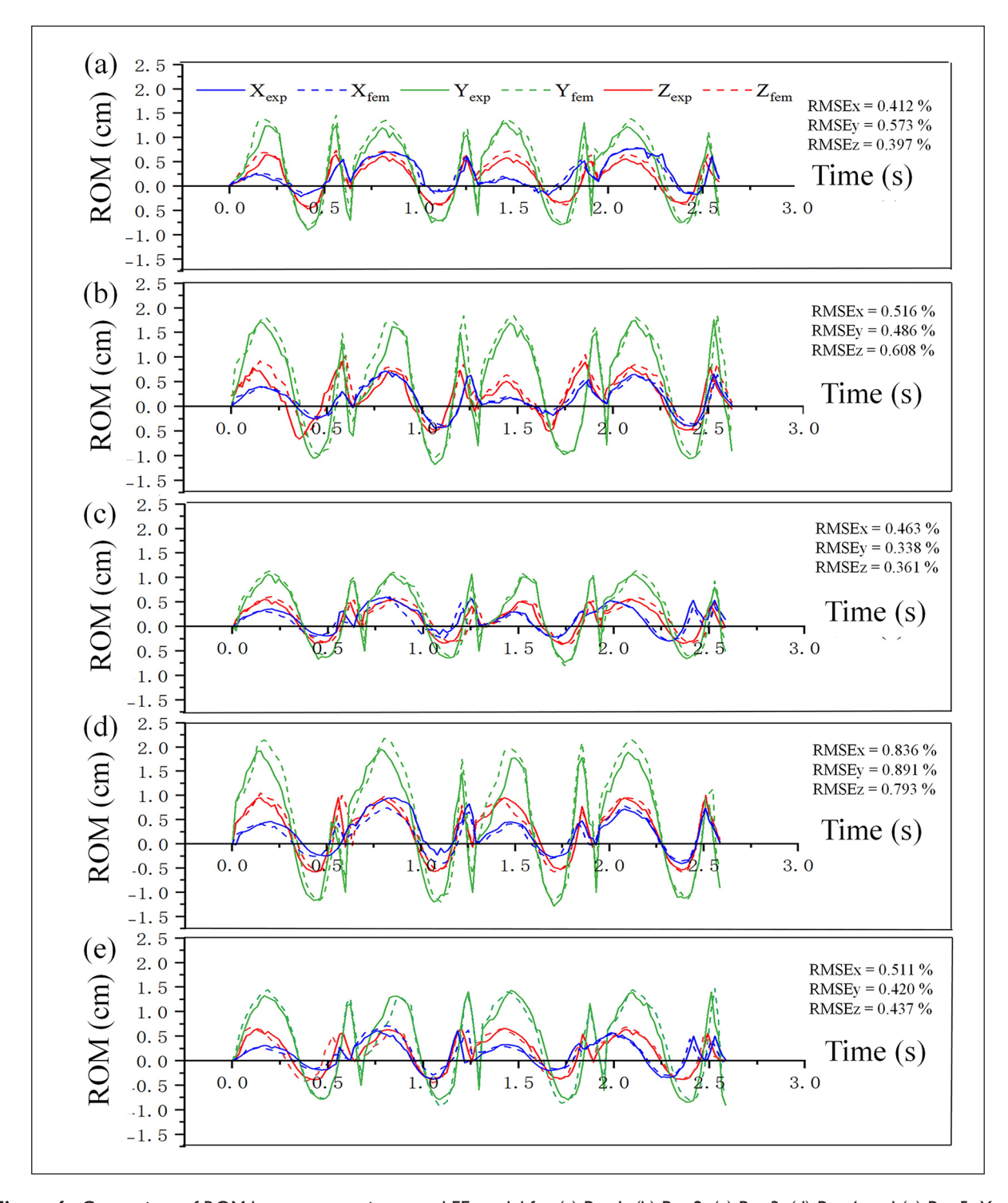


Figure 6. Comparison of ROM between experiment and FE model for (a) Bra 1, (b) Bra 2, (c) Bra 3, (d) Bra 4, and (e) Bra 5. X: anterior-posterior direction, Y: vertical direction, Z: medial-lateral direction.

Table 6. Design matrix of varying modeling parameters and output response.

						Output response						
	Varying levels of design factors					Pressure	Pressure (kPa)			ROM (cm)		
Test No.	С	S _f	S _b	В	U	P _I	P ₂	P ₃	P ₄	ROMx	ROMy	ROMz
I	1	1	1	-1	-1	4.270	2.701	2.248	1.759	0.838	1.729	0.930
2	1	-1	1	-1	I	3.254	2.130	3.690	1.330	1.046	2.018	0.983
3	-1	1	-1	-1	-1	2.820	1.066	1.892	0.738	1.157	2.968	1.525
4	-1	I	-1	I	I	2.983	1.750	3.985	1.250	0.880	1.545	1.010
5	-1	I	I	I	-1	4.076	3.180	2.041	1.240	0.955	2.343	1.333
6	-1	1	-1	-1	I	3.000	1.120	3.660	0.930	0.929	1.771	1.300
7	- 1	-1	-1	-1	I	2.450	1.159	3.845	1.527	1.109	2.739	1.063
8	0	0	0	0	0	3.100	2.130	2.950	1.200	1.032	2.600	1.280
9	-1	-1	-1	I	-1	1.154	1.130	1.625	0.528	1.493	4.126	1.860
10	-1	-1	-1	-1	-1	1.158	0.731	1.724	0.442	1.581	4.628	1.993
П	1	I	-1	I	-1	3.200	1.830	2.216	2.160	0.724	1.750	0.765
12	- 1	1	- 1	- 1	- 1	4.830	3.500	4.268	2.560	0.473	0.279	0.463
13	- 1	1	-1	-1	- 1	3.238	1.370	3.817	1.610	0.694	0.864	0.595
14	i	-1	-1	-1	-1	1.930	0.849	1.801	1.192	1.256	3.633	1.345
15	i	-1	i	-1	-1	2.920	1.990	1.806	1.229	1.153	3.087	1.366
16	-1	-1	i	-1	i	2.672	2.260	3.903	0.776	1.390	3.332	1.630
17	-i	-1	i	i	i	2.557	2.860	3.927	0.940	1.242	2.930	1.500
18	0	0	0	0	0	2.930	2.030	3.100	1.310	1.113	2.437	1.120
19	-1	-1	-1	-1	Ī	1.301	0.681	3.428	0.443	1.393	3.360	1.710
20	i	-i	-i	i	-i	2.246	1.550	2.104	1.750	1.320	3.471	1.319
21	-1	-i	i	i	-i	2.464	2.870	2.049	1.092	1.514	4.197	1.827
22	-I	i	i	i	i	4.339	3.270	4.039	1.290	0.758	1.208	1.050
23	i	-i	i	i	-i	3.206	2.950	2.158	1.790	1.199	3.135	1.240
24	-i	-i	i	-i	-i	1.938	1.741	1.668	0.378	1.477	4.016	1.913
25	i	i	i	-i	i	4.524	2.630	3.932	1.690	0.671	0.440	0.500
26	-i	-i	-i	i	i	1.797	1.770	4.142	1.120	1.296	3.563	1.684
27	i	-1	i	i	i	3.649	3.058	4.156	1.910	1.007	2.000	0.957
28	0	0	0	0	0	2.770	1.890	2.790	1.450	1.063	2.261	1.219
29	-1	Ĭ	Ĭ	-1	-1	3.970	2.350	2.031	0.847	1.152	2.570	1.445
30	i	i	-i	i	i	3.174	1.800	4.214	2.440	0.576	0.615	0.542
31	i	i	i	i	-i	4.677	3.200	2.270	2.510	0.690	1.414	0.686
32	i	i	-i	-i	-i	2.875	1.100	1.973	1.542	0.800	1.977	0.878
33	i	-i	-i	i	i	2.770	1.500	4.101	1.950	1.074	2.336	1.037
34	-1	_, 	-I	i	-i	2.770	1.691	1.987	1.090	1.059	2.680	1.373
35	-1	i	-1	-1	-1	4.303	2.450	4.015	1.076	0.870	1.611	1.163

C, S_p, S_b, B, U: Young's modulus of the cup, front strap; back strap, back panel, and under-band; P₁, P₂, P₃, P₄: dynamic peak pressure at Point1, 2, 3, 4; ROMx, ROMy, ROMz: breast displacement in direction X, Y, Z.

The regression model could be used to estimate the performance metrics of the dynamic peak pressure and ROM for sports bras with respect to different combinations of young's modulus in five parts through a numerical simulation before putting the design into production, and modify the elasticity distribution design based on the output performance and customers' demand.

As shown in Table 7, each output response was significant (p < 0.001), with the R-Sq and R-Sq (adj) above 95%,

no curvature or lack of fit (p > 0.05), as a result, the model was acceptable. ⁴⁴

Ranking of varying factors

Due to the different ranges of varying factors, the strength of their influence could not be read directly in the regression model above. Therefore, varying factors were transformed into dimensionless data, and the normalized

Output response	Sig. (P)	R-Sq (%)	R-Sq(adj) (%)	Curvature (P)	Lack of fit (P)
P.	0.000****	97.83	97.26	0.471	0.634
P ₂	0.000***	97.81	97.34	0.908	0.553
P,	0.000***	98.51	98.25	0.867	0.744
P_{4}^{3}	0.000***	95.94	95.07	0.724	0.599
$\overrightarrow{ROM}x$	0.000***	98.25	97.88	0.589	0.602
ROMy	0.000***	98.79	98.58	0.849	0.800
ROMz	0.000***	98.78	98.56	0.698	0.933

Table 7. Fitting parameters summary of the regression model.

sensitivity factor (φ_n) , calculated by formular (13–14), was taken to evaluate the strength of the effect of Young's modulus of different parts and their interactions on the dynamic peak pressure and breast displacement.^{24,45}

$$\varphi = \frac{1}{2} \left(\frac{\sum \Omega_i^{(+)}}{N/2} - \frac{\sum \Omega_j^{(-)}}{N/2} \right)$$
 (13)

$$\varphi_n = \frac{\varphi}{|\varphi_{max}|} \tag{14}$$

Where, φ is the sensitive factor, calculated by $\sum \Omega_i^{(+)} / (N/2)$ and $\sum \Omega_j^{(-)} / (N/2)$, which is the average value of all results of the output responses at the high or low levels of one factor. φ_n denotes the normalized sensitive factor, φ_{max} is the largest φ to one certain response output. For example, to assess the influence of the Young's modulus of front strap (S_f) on the dynamic peak pressure of Point 1 (P₁), the average value of 16 cases with high Young's modulus (+1) of front strap was calculated as 3.668 kPa, while the average value of the other 16 cases with a low Young's modulus (-1) was calculated as 2.342 kPa. Consequently, the sensitivity factor φ was calculated as 0.663, which was also the φ_{max} to P₁. Then the factors and their interactions for P₁ were normalized in accordance with 0.663, for example, the sensitive factor of C (=0.321) was divided by 0.663, and normalized as 0.451. Furthermore, φ_n was ranked and compared to show the influence of Young's modulus of five parts and their interactions on the dynamic peak pressure and the breast displacement (Figures 7 and 8).

Ranking for dynamic peak pressure. Figure 7 showed the order of the influence strength of Young's modulus of five parts on the dynamic peak pressure of four test points. S_p with the largest normalized sensitivity factor ($\varphi_n = 1$), exhibited the most significant influence on P_1 , followed by S_b (0.902), C (0.484), U (0.261), S_f C (-0.213), and S_f S_b (0.161), while B exhibited the least significant influence

(0.137). For P_2 , three most significant influential factors were S_b (1.000), B (0.525), and S_f (0.261) in a descending order, followed by C and U (φ_n =0.109 for both of them), while the least significant influential factor was S_bB (0.077). For P_3 , U exhibited rather significant influence (1.000), in sharp contrast with other factors, which showed little influence (0.054 ~ 0.122). The most significant influential factor on P_4 was C (1.000), followed by B (0.548) and S_f (0.429), while U (0.173), CB (0.154), and S_b (0.115) show least significant influence.

The results indicated that Young's modulus of five parts and their interactions showed different influence for each test point. P₃ was mainly influenced by Young's modulus of the under-band, rather than Young's modulus of other parts. This might be caused by the special structure of the under-band, forming a circle around the under-bust and mainly stretched in course direction after wearing, which was not easily influenced by Young's modulus of other parts. Similarly, Young's modulus of the under-band exerted little influence on other test points. Except P₃, the dynamic peak pressure of the other three test points was greatly influenced by Young's modulus of the part covering the test point and the parts nearby, but less influenced by Young's modulus of the parts far away from it. For example, the most significant influential factor on P₄ was Young's modulus of cup (C) and the back panel (B), that is, the part covering the breast and the part near Point 4 (in the lower-lateral part of the breast). Nevertheless, Young's modulus of back strap (S_b), which was far away from Point 4, showed the weakest influence. The results might have been due to the fact that the variation in Young's modulus of a certain part would make the stretching of that part and the parts nearby varied, resulted in different elongation and thus variation in pressure, which was also observed in previous researches. 19,21

Ranking for breast displacement. In view of the normalized sensitivity factors in Figure 8, S_f showed the most significant influence (-1.000) on ROM_x, followed by C (-0.616), and U (-0.402), whereas B (-0.170), S_b (-0.122) and S_fB (-0.100) showed less significant influence. For ROM_y, the

^{.100.0 &}gt; q***

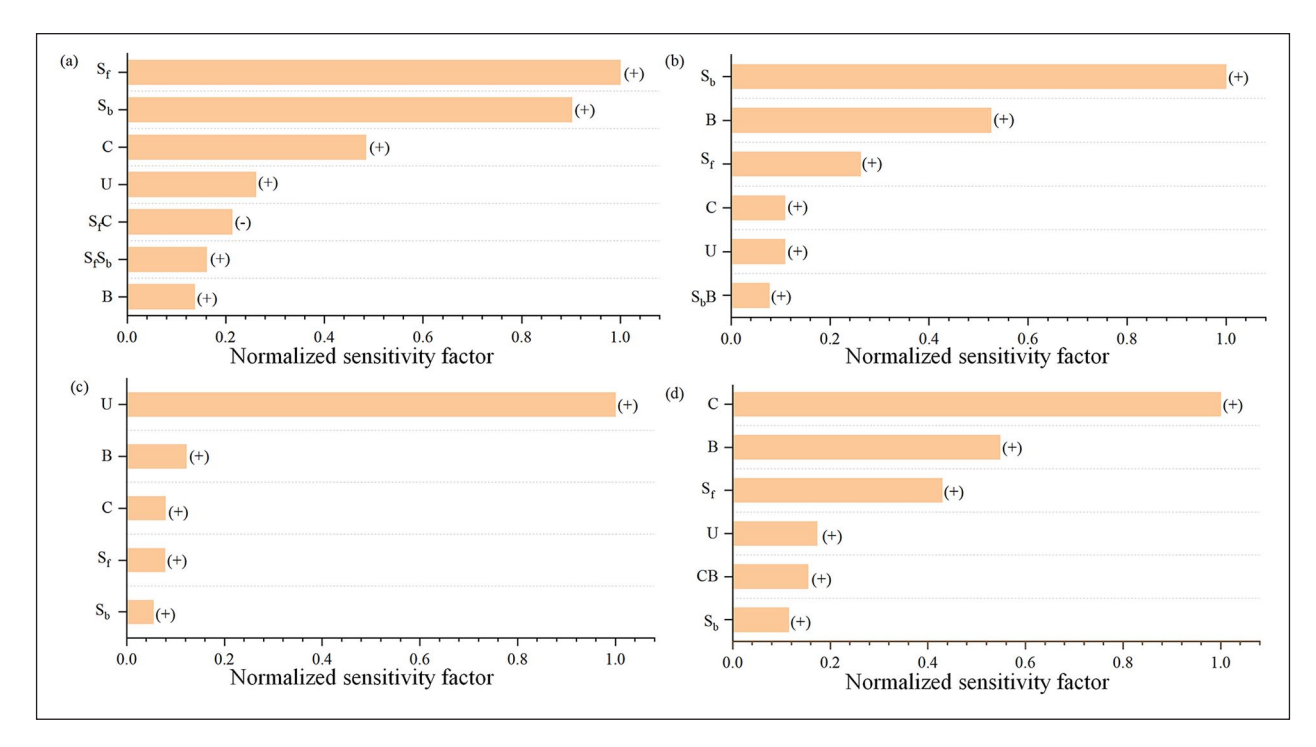


Figure 7. Ranking of varying parameters for sensitivity to: (a) P_1 , with respect to $|\varphi_{S_f}| = 0.663$, (b) P_2 , with respect to $|\varphi_{S_b}| = 0.689$, (c) P_3 , with respect to $|\varphi_{C}| = 0.985$, and (d) P_4 , with respect to $|\varphi_{C}| = 0.462$.

most influential factor was S_f (-1.000), followed by U (-0.638) and C (-0.573), while S_b (-0.214) and B (-0.118) exhibited the least significant influence. Apart from C (-1.000), ROM $_z$ was also significantly affected by S_f (-0.817), followed by U (-0.478), with B (-0.176) and S_b (-0.106) ranked last.

The results revealed the increase of Young's modulus in each part of the sports bra contributed to the reduction of ROM in all three directions. Although the influence of Young's modulus of each part was different on ROM in three directions, S_f, C, and U were always ranked as three most significant factors, whereas S_b and B were the two least significant factors. The results showed consistency with previous researches which implied that applying fabrics with high Young's modulus in cup8 and underband^{18,46} was effective in reducing breast displacement. The fabric tension resulted from the deformation of the cup would reduce the moving of the breast, and the increase of Young's modulus of the under-band exerted higher contact pressure between the under-band and the body, resulting in the reducing of the slip in the underband.²¹ In addition, the effect of Young's modulus of the strap has also been discussed in previous researches, which revealed that increasing Young's modulus contributed to the reducing of breast displacement.¹⁴ However, the differences between the influence of S_f and S_h has yet to be discussed. It was found that ROM was mainly affected by S_f rather than S_h in this study, which may provide novel information for the strap design.

In summary, the elasticity distribution affected both the dynamic peak pressure and ROM in three directions. Besides, the influence strength of Young's modulus of each part varied with the pressure test points and the directions of ROM. Since S_b exhibited strong influence on P₁ and P2, B showed significant influence on P2 and P4, whereas both of them exhibited weak influence on ROM in three directions, fabrics with relatively low Young's modulus were suggested for these two parts in order to improve pressure comfort. Nevertheless, increasing S₂, C, and U were not only effective in reducing ROM, but also contributed to the increase of P₁, P₃, and P₄, resulting in discomfort in these areas. It was found that the pressure comfort threshold (PCT), that is, a feeling boundary between comfort and discomfort, 47 differed between body parts. The top area of the shoulder and the side area covered by the under-band showed higher PCT than the breast area, 48 as a result, fabrics with relatively high Young's modulus may be applied for the front straps and the underband to improve the breast support performance, whereas appropriate fabrics according to the PCT of the breast and the effect in ROM may be chosen for the cup.

Conclusions

This paper analyzed the effects of elasticity distribution on the performance of pressure comfort and breast support of sports bras by applying a two-level factorial design-ofexperiment (DOE) approach based on FE model. A

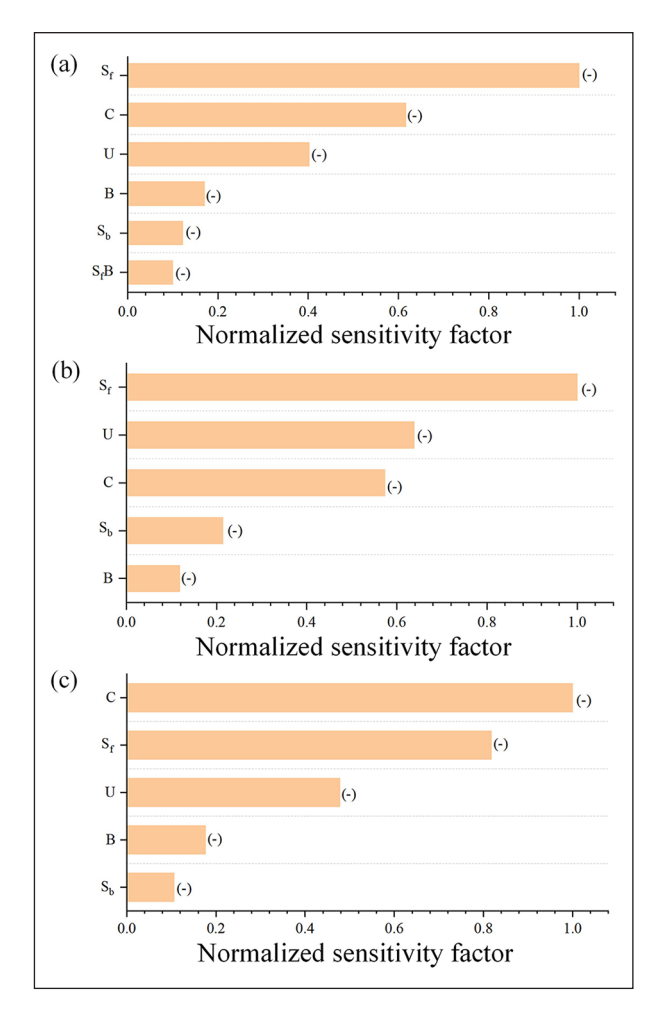


Figure 8. Ranking of varying parameters for sensitivity to: (a) ROMx, with respect to $|\varphi_{S_f}| = 0.229$, (b) ROMy, with respect to $|\varphi_{S_f}| = 0.838$, and (c) ROMz, with respect to $|\varphi_{C}| = 0.301$.

quantitative relationship between Young's modulus of five parts of sports bras and the performance metrics of pressure and breast displacement was explored, based on which, the strength of the influence of these parts were further examined. Regarding the dynamic pressure, the dynamic peak pressure of Points 1, 2, and 4 was primarily influenced by the Young's modulus of the part covering the point and the parts nearby, but less influenced by the Young's modulus of the parts far away from it. Different from them, P₂ covered by the lateral area of the under-band was significantly influenced by the Young's modulus of the under-band, rather than the Young's modulus of other parts. Concerning ROM, S_t, C, and U were ranked as three most significant factors in all three directions, while S_b and B were the two least significant factors. Consequently, it was suggested that applying fabrics with relatively low Young's modulus in back panel and back strap, relatively high Young's modulus in front strap and under-band, and selecting appropriate fabrics for the cup according to PCT of the breast and ROM, to optimize the pressure comfort and breast support performance of sports bras.

These findings provided novel information for optimizing pressure comfort and breast support performance of sports bras, which was supposed to serve as a valuable reference for bra industry. Additionally, similar analysis could be easily extended to other design parameters and performance of the sports bras, such as thermal comfort. Nevertheless, limitations in subjects, samples and experiment motions should be noticed. Future works may involve more subjects with different age, body mass, and breast size, more types of sports bras with different elasticity distribution, and more different motions for experiment to benefit more women in varied exercise. Besides, as the differences in the breast height after wearing different sports bras may affect the simulated results, they will be taken into consideration in future researches to develop a more rigorously validated FE model. Moreover, for simulating efficiency of the FE model, the trunk was simplified to three main parts: the torso, the soft tissue and the breasts, models with more detailed layers of the trunk were needed in future to improve the accuracy of simulation.

ORCID iDs

Xiaofang Liu https://orcid.org/0000-0003-2660-2168 Liling Cai https://orcid.org/0000-0001-9573-6683

Funding

The author(s) disclosed receipt of the following financial support for the research, authorship, and/or publication of this article: 1. General project of philosophy and social science research in Jiangsu universities: Research on the Changes and Digital Activation of Women's Clothing in Southern Jiangsu since the Foundation of People's Republic of China (Grant/Award Number:2024SJYB0423). 2. High-level Talents Research Start-up Project of Jinling Institute of Technology: Effects of Elasticity distribution on pressure and breast displacement for sports bras (Grant/Award Number: jit-b-202368).

Declaration of conflicting interests

The author(s) declared no potential conflicts of interest with respect to the research, authorship, and/or publication of this article.

References

- Scurr JC, White JL and Hedger W. Supported and unsupported breast displacement in three dimensions across treadmill activity levels. *J Sports Sci* 2011; 29: 55–61.
- Burbage J and Cameron L. An investigation into the prevalence and impact of breast pain, bra issues and breast size on female horse riders. *J Sports Sci* 2017; 35(11): 1091–1097
- Brisbine BR, Steele JR, Phillips EJ, et al. Breast pain affects the performance of elite female athletes. *J Sports Sci* 2020; 38(5): 528–533.
- Burnett E, White J and Scurr J. The influence of the breast on physical activity participation in females. J Phys Act Health 2015; 12(4): 588–594.
- Maleki MS, Mahmoudnia S and Mousazadegan F. Influence of weft knitted fabrics tensile characteristics and garment

- size on the body movement comfort. *Indian J Fibre Text Res* 2020; 45(3): 352–358.
- Takasu N, Furuoka S, Inatsugi N, et al. The effects of skin pressure by clothing on whole gut transit time and amount of feces. *J Physiol Anthropol Appl Human Sci* 2000; 19(3): 151–156.
- Chen X, Gho SA, Wang J, et al. Effect of sports bra type and gait speed on breast discomfort, bra discomfort and perceived breast movement in Chinese women. *Ergonomics* 2016; 59(1): 130–142.
- Lu M, Qiu J, Wang G, et al. Mechanical analysis of breast– bra interaction for sports bra design. *Mater Today Commun* 2016; 6: 28–36.
- Wu J, Jin Z, Jin J, et al. Study on the tensile modulus of seamless fabric and tight compression finite element modeling. *Text Res J* 2020; 90(1): 110–122.
- Mori Y, Kioka E and Tokura H. Effects of pressure on the skin exerted by clothing on responses of urinary catecholamines and cortisol, heart rate and nocturnal urinary melatonin in humans. *Int J Biometeorol* 2002; 47(1): 1–5.
- Macintyre L and Baird M. Pressure garments for use in the treatment of hypertrophic scars an evaluation of current construction techniques in NHS hospitals. *Burns* 2005; 31(1): 11–14.
- Lawson L and Lorentzen D. Selected sports bras: comparisons of comfort and support. *Cloth Text Res J* 1990; 8(4): 55–60.
- 13. Bowles KA and Steele JR. Effects of strap cushions and strap orientation on comfort and sports bra performance. *Med Sci Sport Exer* 2013; 45(6): 1113–1119.
- Norris M, Blackmore T, Horler B, et al. How the characteristics of sports bras affect their performance. *Ergonomics* 2021; 64(3): 410–425.
- Liu X, Ji X, Ocran FM, et al. Effects of ventilation design on thermal comfort performance and breast displacement for sports bras. *Text Res J* 2023; 93(3–4): 519–537.
- 16. Zheng R, Yu W, Fan J, et al. Pressure evaluation of 3d seamless knitted bras and conventional wired bras. *Fibers Polym* 2009; 10(1): 124–131.
- 17. Dan R, Fan XR, Xu LB, et al. Numerical simulation of the relationship between pressure and material properties of the top part of socks. *J Text I* 2013; 104(8): 844–851.
- Liu C, Miao FX, Dong XY, et al. Enhancing pressure comfort of a bra's under-band. Text Res J 2018; 88(19): 2250–2257.
- 19. Liu Z, Han X, Zhang Y, et al. Knitting 4d garments with elasticity controlled for body motion. *ACM Trans Graph* 2021; 40(4): 1–16.
- 20. Li H, Wang Y and Chen Z. Evaluation on the pressure distribution and body-shaping effectivity of graduated compression shaping pants. *Int J Clothing Sci Technol* 2020; 33(2): 153–162.
- 21. Liu XF, Ji XF, Yan YX, et al. The elasticity distribution of under-band based on pressure comfort and breast support performance for seamless sports bras. *Ind Textila* 2023; 71(3): 278–285.
- Mills C, Ayres B and Scurr J. Breast support garments are ineffective at reducing breast motion during an aqua aerobics jumping exercise. *J Hum Kinet* 2015; 46: 49–58.
- 23. Norris M, Jones M, Mills C, et al. The kinematics of breasts implanted with a reduced mass implant: a pilot study. *Aesthet Surg J* 2020; 40(5): n253–n262.

- Zhang S, Yick KL, Chen L, et al. Finite-element modelling of elastic woven tapes for bra design applications. *J Text Inst* 2020; 111(10): 1470–1480.
- Sun Y, Chen LH, Yick KL, et al. Optimization method for the determination of Mooney-Rivlin material coefficients of the human breasts in-vivo using static and dynamic finite element models. *J Mech Behav Biomed* 2019; 90: 615–625.
- Chen J, Sun Y, Liu Q, et al. Construction of multi-component finite element model to predict biomechanical behaviour of breasts during running and quantification of the stiffness impact of internal structure. *Biomech Model Mechanobiol* 2024; 23(5): 1679–1694.
- Sun Y, Yick KL, Cai Y, et al. Finite element analysis on contact pressure and 3D breast deformation for application in women's Bras. *Fibers Polym* 2021; 22(10): 2910–2921.
- Liang RX, Yip J, Yu W, et al. Numerical simulation of nonlinear material behaviour: application to sports bra design. *Mater Des* 2019; 183: 1–7.
- 29. Li Y, Zhang X and Yeung KW. A 3d biomechanical model for numerical simulation of dynamic mechanical interactions of bra and breast during wear. *Sen i Gakkai* 2003; 59(1): 12–21.
- Sun Y, Yick KL, Yu W, et al. 3D bra and human interactive modeling using finite element method for bra design.
 Comput Aided Des 2019; 114: 13–27.
- 31. Gao YM. Research in breast morphology and bra structure of older women between 60 and 75 years old. Wuhan: Wuhan Textile University, 2020 (Chinese).
- Zhang S, Yick KL, Yip J, et al. An understanding of bra design features to improve bra fit and design for older Chinese women. *Text Res J* 2021; 91(3–4): 406–420.
- Risius D, Milligan A, Berns J, et al. Understanding key performance indicators for breast support: an analysis of breast support effects on biomechanical, physiological and subjective measures during running. *J Sports Sci* 2017; 35(9): 842–851.
- 34. Yan Y, Gao J, Jin Z, et al. Research on the relationship between clothing pressure developed by women's basketball sports bra and heart rate variation indexes. *Int J Clothing Sci Technol* 2014; 26(6): 500–508.
- Coltman CE, Steele JR and McGhee DE. Effects of age and body mass index on breast characteristics: A cluster analysis. *Ergonomics* 2018; 61(9): 1232–1245.
- Central Committee of the Communist Youth League. More than 100 million people, why do Chinese love square dancing so much? Online Referencing, https://baijiahao.baidu. com/s?id=1651341098880763499&wfr=spider&for=pc (2019, accessed 27 November 2019).
- Coltman CE, McGhee DE and Steele JR. Bra strap orientations and designs to minimise bra strap discomfort and pressure during sport and exercise in women with large breasts.
 Sports Med 2015; 1: 21–28.
- 38. McLean AR, Richards ME, Crandall CS, et al. Ultrasound determination of chest wall thickness: implications for needle thoracostomy. *Am J Emerg Med* 2011; 29(9): 1173–1177.
- Zhang J, Lau NM, Sun Y, et al. Non-linear finite element model established on pectoralis major muscle to investigate large breast motions of senior women for bra design. *Text Res J* 2022; 92(19–20): 3511–3521.

- 40. Eder M, Raith S, Jalali J, et al. Comparison of different material models to simulate 3-D breast deformations using finite element analysis. *Ann Biomed Eng* 2014; 42(4): 843–857.
- 41. Ruixin L, Yip J, Yu W, et al. Computational modelling methods for sports bra–body interactions. *Int J Clothing Sci Technol* 2020; 32(6): 921–934.
- Cai Y, Yu W, Zhou J, et al. A piecewise mass-spring-damper model of the human breast. *J Biomech* 2018; 67: 137–143.
- 43. Hodgson JA, Chi SW, Yang JP, et al. Finite element modeling of passive material influence on the deformation and force output of skeletal muscle. *J Mech Behav Biomed Mater* 2012; 9: 163–183.
- 44. Douglas CM. *Design and analysis of experiments*. 4th ed. Wiley, 1997.

- 45. He Z and Dass ETM. Correlation of design parameters with performance for electrostatic precipitator. Part ii. Design of experiment based on 3d fem simulation. *Appl Math Model* 2018; 57: 656–669.
- Zhou J, Yu W and Ng SP. Identifying effective design features of commercial sports bras. *Text Res J* 2013; 83: 1500–1513
- Wang Y, Liu Y, Luo S, et al. Pressure comfort sensation and discrimination on female body below waistline. *J Text Inst* 2018; 109(8): 1067–1075.
- 48. Kim SPN and Lee KHY. Clothing pressure, blood flow, and subjective sensations of women in their 50s and 60s when wearing a commercial yoga bra top. *J Korean Soc Clothing Text* 2021; 45(4): 86–97.